

# Nail Abnormalities Identified in an Aging Study of 30 Inbred Mouse Strains

Sarah C. Linn<sup>1\*</sup>, Allison M. Mustonen<sup>2\*</sup>, Kathleen A. Silva<sup>3</sup>, Victoria E. Kennedy<sup>3</sup>,  
Beth A. Sundberg<sup>3</sup>, Lesley S. Bechtold<sup>3</sup>, Sarah Alghamdi<sup>4</sup>, Robert Hoehndorf<sup>4</sup>,  
Paul N. Schofield<sup>3,5</sup> and John P. Sundberg<sup>3</sup>

<sup>1</sup>The Ohio State University College of Veterinary Medicine, Columbus, OH, USA; <sup>2</sup>Purdue University College of Veterinary Medicine, West Lafayette, IN, USA; <sup>3</sup>The Jackson Laboratory, Bar Harbor, ME, USA, <sup>4</sup>Computational Bioscience Research Center, King Abdullah University of Science and Technology, Thuwal, Kingdom of Saudi Arabia; and <sup>5</sup>Department of Physiology Development and Neuroscience, University of Cambridge, Downing Street, Cambridge CB2 3EG, UK.

\*Equal work; work done during an externship at The Jackson Laboratory

**Corresponding author:** John P. Sundberg, D.V.M., Ph.D., The Jackson Laboratory, 600 Main Street, Bar Harbor, ME 04609-1500 USA  
Phone: 207-288-6410  
FAX: 207-288-6077  
Email: john.sundberg@jax.org

**Key words:** nail dystrophy, pododermatitis circumscripta, subungual intraosseous epidermoid inclusion cysts

**Article type:** Regular Article

**Running head:** Old mouse nails

**Acknowledgements:** The authors thank Zoe Reifsnnyder in JAX Creative for assistance with preparation of the figures. This work was supported by American Hair Research Society Mentorship Grants (to SL and AM); Ellison Medical Foundation (to JPS); and the National Institutes of Health (AG025707, for the Shock Aging Center). The Jackson Laboratory Shared Scientific Services were supported in part by a Basic Cancer Center Core Grant from the National Cancer Institute (CA034196).

**Contribution of authors:** SCL, AMM, and JPS wrote the manuscript; SCL, AMM, JPS, KAS, VEK, and BAS did the research and data analyses; LSB did the scanning electron microscopy; and SA, RH, and PNS did the statistical analyses. All authors reviewed and edited the manuscript.

**Conflicts of interest:** JPS serves on an advisory board for Bioniz. JPS, KAS, and VEK do sponsored research with Biocon, Takeda, and Theravance, none of which has any relevance to the work reported here. All other authors report no conflicts of interest.

**Abstract:**

In a large scale aging study, 30 inbred mouse strains were systematically screened for histologic evidence of lesions in all organ systems. Ten strains were diagnosed with similar nail abnormalities. The highest frequency was noted in NON/ShiLtJ mice. Lesions identified fell into two main categories: acute to chronic penetration of the third phalangeal bone through the hyponychium with associated inflammation and bone remodeling or metaplasia of the nail matrix and nail bed associated with severe orthokeratotic hyperkeratosis replacing the nail plate. Penetration of the distal phalanx through the hyponychium appeared to be the initiating feature resulting in nail abnormalities. The accompanying acute to subacute inflammatory response was associated with osteolysis of the distal phalanx. Evaluation of young NON/ShiLtJ mice revealed that these lesions were not often found, or affected only one digit. The only other nail unit abnormality identified was sporadic subungual epidermoid inclusion cysts which closely resembled similar lesions in human patients. These abnormalities, being age-related developments, may have contributed to weight loss due to impacts upon feeding and should be a consideration for future research due to the potential to interact with other experimental factors in aging studies using the affected strains of mice.

## Introduction:

The nail unit is a complex anatomic structure in mammals. Although diseases of the nail unit may occur concurrently with a variety of skin diseases in humans, the details of many of these diseases are rarely reported because detailed biopsies (sagittal sections) are available only at the time of autopsy or digital amputation. While, superficially, human nails appear to differ from those of laboratory mice, primarily due to the human nail being a slightly curved plate compared to a laterally compressed curved, almost conical structure in the mouse, microscopically all layers are quite similar.(1) The mouse nail plate, being quite small and difficult to evaluate without magnification, is often overlooked in phenotyping studies of new mutations. This is complicated at the histological level due to differential textures of the distal phalangeal bone, soft tissues, and nail plate, which makes sectioning difficult resulting in poor quality or non-diagnostic slides.

A variety of abnormalities have been described in mice including long curled nails in animals carrying mutations in the hairless (*Hr*) gene and its genocopies (2-4), nail plate abnormalities with separation from the nail bed in some but not all strains of mice with alopecia areata (5), thin nail plates in nude mice (*Foxn1<sup>mu</sup>*)(6) or bone morphogenic protein receptor, type 1A (*Bmpr1a<sup>tm2.1Bhr</sup>*) (7, 8), destruction of the entire nail unit by trauma in sensory deprivation syndrome, such as mice with null mutations in the nerve growth factor receptor gene (*Ngfr*, formerly called *p75*) (4), and many other phenotypes. In most cases, abnormalities can be observed in young mice through adulthood affecting all nails on both front and rear feet. Spontaneously occurring nail abnormalities in the most commonly used inbred mouse strains, particularly in old mice, have not been described. Understanding abnormal phenotypes that regularly occur associated with specific mutations in mice or in specific inbred strains are critical to avoid misinterpretations of experimentally induced lesions.

In a large scale aging study of 30 inbred strains, nail plate dystrophy with or without perforation of the hyponychium by the third phalangeal bone was observed sporadically in 9 strains and frequently in NON/ShiLtJ mice. We describe here the epidemiology, clinical, and pathologic features of these lesions and progression of this disease. Incidental, sporadic, subungual epidermoid inclusion cysts, identical to a similar lesion sporadically seen in humans and other mammals, were the only other nail-related lesions observed.

## Materials and Methods:

Mice. 129S1/SvImJ, A/J, AKR/J, BALB/cByJ, BTBRT<sup>+</sup>*tf*/J, BUB/BnJ, C3H/HeJ, C57BL/10J, C57BL/6J, C57BLKS/J, C57BR/cdJ, C57L/J, CAST/EiJ, CBA/J, DBA/2J, FVB/NJ, KK/HIJ, LP/J, MRL/MpJ, NOD.B10Sn-H2<sup>b</sup>/J (a congenic strain with the NOD genetic background but with a histocompatibility locus from a diabetes-resistant strain), NON/ShiLtJ, NZO/HILtJ, NZW/LacJ, P/J, PL/J, PWD/PhJ, RIIS/J, SJL/J, SM/J, SWR/J, and WSB/J were obtained from The Jackson Laboratory (Bar Harbor, ME). Three of the strains were not evaluated at all time points because of lymphoma development (AKR/J), lack of sufficient mice for analysis (CAST/EiJ), or self-mutilations resulting in euthanasia for humane purposes (SJL/J). (9, 10) Taken together the strains selected were genetically diverse, which was estimated by SNP genotyping of over 100 strains into 7 distinct genetic groups, so that there were 3-7 strains representing each of the groups.(11)

Husbandry. Mice in the aging study were maintained in an humidity-, temperature-, and light cycle (12:12 hrs) controlled vivarium under specific pathogen-free conditions

(<https://www.jax.org/jax-mice-and-services/customer-support/customer-service/animal-health/health-status-reports>). Mice were housed in double-pen polycarbonate cages (330 cm<sup>2</sup> floor area) at a maximum capacity of four mice per pen. Mice were allowed free access to autoclaved food (NIH 31, 6% fat; Lab Diet 5K52, Purina Mills, St. Louis, MO) and acidified water (pH 2.8–3.2).

**Study Design.** Mice were evaluated either in longitudinal (life-span) or cross-sectional studies to identify diseases at 12 and 20 months. Longitudinal study mice were euthanized by CO<sub>2</sub> asphyxiation only after becoming moribund following conditions approved by The Jackson Laboratory Institutional Animal Care and Use Committee.(9) A total of 96 mice per strain were used for the animals involved in the longitudinal study in order to provide statistical significance in detecting a 10% difference in lifespan. Age-related physiological phenotypes were assessed for each strain every 6 months in addition to lifespan.(12)

Mice involved in the cross sectional study were euthanized by CO<sub>2</sub> asphyxiation in cohorts at 12 months +/- 28 days and 20 months +/- 28 days. Fifteen females and fifteen males were aged and those that survived to 12- and 20-months of age (total of 60 animals per strain) were euthanized and complete necropsies were performed.(13) In these studies, the left rear leg was collected to evaluate the joints and nail unit. One to 3 nails were evaluated per mouse using hematoxylin and eosin stained sagittal sections (13) in 1,668 mice 12 months of age and older. NON/ShiLtJ mice were found in the histopathological screen to have a high frequency of nail unit abnormalities. To determine if these lesions occurred in younger mice, 7 females and 7 males, 57-241 days of age (2-8 months of age), were obtained from The Jackson Laboratory production colonies.

**Tissue collection.** All major tissues were collected at the time of necropsy and were fixed by immersion in Fekete's acid-alcohol-formalin solution.(10, 13) Left front and rear feet were removed at the carpal/metacarpal and tarsal/metatarsal joints, respectively and placed into Fekete's acid-alcohol-formalin. The bones were processed in Cal-Ex® (Fisher, Pittsburgh, PA) for 24 hours after fixation and then transferred to 70% ethanol, trimmed, processed routinely, embedded in paraffin, sectioned at 6 µm, and stained with hematoxylin and eosin (H&E). These tissues included longitudinal sections of the front and rear foot (soft tissues, bone, and nail unit/footpad).

**Immunohistochemistry.** Mouse specific keratins 1 and 10 are differentially expressed in the epidermis and foot pad but not in the nail matrix or nail bed (1) and were therefore used to evaluate changes in the old mouse nail unit. Antibodies used on serial sections of digits (KRT1, stock# PRB-165P (1:100) and KRT10, stock# PRB-159P (1:100); Covance, Berkeley, CA), including the nail unit, were obtained from a 395 day old SWR/J female with a normal nail unit, 204 day old male NON/ShiLtJ with subacute inflammation of one nail unit due to perforation and a second normal nail unit, and a 620 day old female with severe nail dystrophy and acute inflammation of the underlying connective tissue. More information is available on the Mouse Tumor Biology Database website (<http://tumor.informatics.jax.org/html/antibodies.html>). Immunohistochemistry was done using a Ventana Discovery XT autostainer (Tucson, AZ). Diaminobenzidine (Sigma, St. Louis, MO) was used as chromogen.

Scanning Electron Microscopy (SEM). Right front and rear feet were removed from selected mice that were also used for histologic evaluation. Feet were fixed overnight at 4°C in 2.5% glutaraldehyde in 0.1 M phosphate buffer (pH 7.2). After rinsing the tissues several times in phosphate buffer, they were post-fixed in 1% osmium tetroxide in phosphate buffer for 48 hr at 4°C and dehydrated in a graded series of ethanol (40%, 60%, 80%, 95%, and 100% ethanol, each for an hour at room temperature). Critical point drying was done by gently flushing specimens four times with CO<sub>2</sub> for 5 min while gradually increasing temperature in the critical point drier (Balzers, Union, FL) to 41°C. Over a period of 30–40 min, pressure was released slowly to allow CO<sub>2</sub> to evaporate while allowing the sample to return to room temperature. Feet were mounted on aluminum stubs using double-sided carbon tape and sputter-coated with a 4 nm layer of gold. Nails were examined at 20 kV at a working distance of  $\approx$ 5 mm on a Hitachi S3000N VP Scanning Electron Microscope (Hitachi Science Systems, Japan).(6, 14)

Data management. Slides for this study were reviewed by a board-certified veterinary pathologist (JPS).(9) Diagnoses were entered into a relational database, the Mouse Disease Information System (MoDIS), using the mouse anatomy ontology (MA) to code for the organ and the mouse pathology ontology (MPATH) to code for the disease process (diagnosis).(15) A severity score was recorded (0, normal; 1, mild; 2, moderate; 3, severe; or 4, extreme) to account for differences in the size, severity, and biological behavior of lesions, based on standard criteria used by pathologists. Using MoDIS, strains with any abnormalities of the nail unit were identified and all slides of the digits were retrieved and reviewed. Sections that were not of diagnostic quality in the most affected strain (NOD/ShiLtJ) were recut.

Statistical Analysis. 1326 mice were scored at 12 and 20 months of age for pathological lesions, of these 53 were NON/ShiLtJ. The average number of mice per strain was 44, min 16, max 59 with 30 strains in all. Mice were coded to MA(16) and MPATH(17) ontology terms as described above. A combined enrichment analysis was performed over observed pathological lesions (from MPATH) and anatomical location of the lesion (from MA). MPATH and MA were combined into a single ontology using Description Logic axioms; specifically, given a lesion L affecting the anatomical site S, a new class is generated combining both, defined as `equivalent_to "L and affects_some (part-of some S)"`. The HeRMIT reasoner (18) was then used to infer the hierarchical structure of the combined ontology and the OntoFunc tool (19) used to generate a structure suitable for enrichment analysis with Func.(20) A hypergeometric test was then conducted comparing one strain with all other strains. This test was repeated for several groups of mice: all mice at age 12 months, all mice at age 20 months, and the same time points separated by sex. Enriched classes (combinations of pathological lesion and anatomical site, e.g. (Nail+Dystrophy)) were identified after multiple testing correction for false discovery rate.(21) Sexual dichotomy for dystrophic lesions was calculated using Fishers Exact test.

## **Results:**

### Nail Dystrophy in Mouse Strains.

Most nail units in mice in this study were normal (**Fig. 1**). On average, 40% of the slides with digits did not include the nail unit. The nail unit was out of the section or, due to textural differences with the surrounding tissue and paraffin, it was pulled out of the section by the microtome. All digits from NON/ShiLtJ mice that did not have nails of diagnostic quality were recut which enabled half to be diagnostic. Lesions were recorded only for mice that had nail

units that could be evaluated. Ten of the 30 inbred mouse strains evaluated in the aging study had the nail abnormality with NON/ShiLtJ and NZW/LacJ representing the most frequently affected strains (**Supplemental Fig. 1, Table 1**). All affected strains had similar lesions. Ontology-driven overrepresentation analysis indicated that NON/ShiLtJ showed disproportionately more inflammatory and dystrophic lesions with respect to all other strains both at 12 ( $p=5.9e-5$  and  $p=1.0e-11$  respectively) and 20 months of age ( $p=1.1e-7$  and  $p=1.2e-9$  respectively), with a significance cut-off at  $p=0.05$ . NZW/LacJ showed significance at  $p=0.028$  for nail dystrophy in females at 20 months. Furthermore, all mice in the family tree Group 3 had multiple individuals with these nail abnormalities (**Supplemental Table 1**).

In general, lesions fell into two categories. Acute to chronic penetration of the third phalangeal bone (P3) through the hyponychium with associated inflammation and bone remodeling, or metaplasia of the nail matrix and nail bed was associated with severe orthokeratotic hyperkeratosis replacing the nail plate (**Fig. 2**).

Evaluation of additional, younger NON/ShiLtJ mice, 57-241 days of age, revealed that these lesions were not found in the very young mice but as they aged, one or more of the nail units became affected indicating that these changes were age related. Early lesions helped define the time course of the disease process. Perforation of the hyponychium appeared to be the first stage as the nail matrix and nail plate were largely unaffected histologically. The acute perforation was associated with desiccation of the attached, exposed soft tissues. If the defect was small, there was acute inflammation, hemorrhage, and bacterial colonization. More severe penetration resulted in severe hemorrhage and serum exudation that extended under the nail plate creating pressure that led to necrosis of the nail bed and matrix (**Fig. 2**). Osteolysis of P3 resulted in nearly complete loss of P3 in some cases. Re-epithelialization appeared to occur from either end of the denuded area, either from the proximal nail fold or hyponychium, resulting in metaplasia (markedly cornified stratified squamous epithelium more similar to the epidermis than the matrix) thereby closing the defect.

Immunohistochemistry for mouse specific acid-base, heteroduplex keratins 1 (KRT1) and 10 (KRT10) both labeled the suprabasilar, terminally differentiated keratinocytes of the proximal nail fold epidermis and of the hyponychium but not the normal nail matrix or bed.(1) The epithelium that replaced these structures in the NON/ShiLtJ mice with abnormal nails resembled epidermis or hyponychium. However, expression of KRT1 or KRT10 was only present partially extending from the proximal nail fold into the proximal matrix at the junction (data not shown).

#### Scanning Electron Microscopy and Elemental Analysis.

Scanning electron microscopy (SEM) is a useful tool for visualizing the nail and to confirm to confirm nail plate dystrophy.(6) NON/ShiLtJ mice, 57-241 days of age, were evaluated and found to be similar to C57BL/6J controls at the younger ages at low magnification. Older mice had one or more affected digits which ranged from an abnormal hyponychium to healed, but missing, amputated distal digits (**Fig. 3A, B**). Nail plates in the C57BL/6J control mice (309 days of age) had well-formed, flattened squames on the lateral edges (**Fig. 3C**) compared to irregular to linear patterns in the older NON/ShiLtJ mice (211 days and older; **Fig. 3D**) suggesting a primary nail plate abnormality existed.

#### Subungual intraosseous epidermoid cysts.

Eight cases (0.48%) had subungual intraosseous epidermoid cysts that would not have been detected without histologic screening. Affected strains included 129S1/SvImJ, BALB/cByJ,

C57L/J, FVB/NJ, LP/J, and MRL/MpJ (**Supplemental Table 1**) ranging from 377-882 (675 mean) days of age. Two females and 6 males were affected.

Mice with epidermoid inclusion cysts did not exhibit any clinical abnormalities to suggest there were digital abnormalities. In all cases the basic nail unit was intact with no evidence of trauma. The nail plate was intact and there was no evidence of fibrosis or inflammation under the nail bed that would suggest trauma. The nail bed was relatively normal or mildly hyperplastic associated with arborizing extensions of keratinocytes into the underlying connective tissue. These downward proliferations were very prominent (**Fig. 4. A, B**), short and subtle (**Fig. 4. C, D**), or not obvious in the section examined (**Fig. 4. E, F**). Most formed cystic structures filled with laminated cornified material (**Fig. 4. C-E**), the largest of which was 200  $\mu\text{m}$  in diameter, while others had few or no cysts (**Fig. 4. A, B**). The underlying distal phalangeal bone (P3) is normally triangular in shape, pointed at the most distal end, with a marrow cavity.(1) In all but one of these cases, P3 underwent various degrees of remodeling as these epidermoid cysts extended into the bone. Lesions were very small in the one case without bone involvement (data not shown).

### **Discussion:**

Penetration of the distal phalanx through the hyponychium appeared to be the initiating feature of nail unit abnormalities in old mice affecting multiple, but not all strains. The accompanying acute inflammatory response was associated with osteolysis of the distal phalanx. Bone penetration was a consistent feature in affected young NON/ShiLtJ mice with normal appearing nail plates. The nail plate and matrix were separated and compressed by the penetrating bone and hemorrhage separating the nail bed from the nail plate resulting in necrosis of the nail matrix and bed. In response to the damage, stem cells from the basal layer of the proximal nail fold or hyponychium proliferated and covered the injury(8) resulting in metaplasia to a markedly cornified and hyperplastic epithelium. Keratins 1 and 10, not normally expressed in the matrix or nail bed, were not expressed in the epithelium that replaced the nail bed but did extend into the proximal nail matrix suggesting there was a metaplastic response to heal the injury.

All aged mice in this study were housed in the same barrier facility at the same time under the same conditions including food, water, and pathogen free conditions. If this were simply a husbandry issue, lesions would be expected to occur in a random, low frequency manner, which was not the case. Food was located in a metal hopper that the mice had to access, which may have been a potential source of trauma. Discussions with investigators using NON/ShiLtJ mice did not indicate any unusual behavior of these mice compared with other strains commonly used for diabetes research (David Serreze, The Jackson Laboratory, personal comments). NON/ShiLtJ (nonobese nondiabetic) mice are often used as controls for the NOD/ShiLtJ (nonobese diabetic mice) in diabetes studies. As stated in the materials and methods, NOD.B10Sn-*H2<sup>b</sup>*/J, a congenic strain with the NOD genetic background but with a histocompatibility locus from a diabetes-resistant strain, were used in this study to reduce any effect of diabetes on longevity.

One third of the strains were affected. Overrepresentation analysis showed that NON/ShiLtJ and NZW/LacJ strains had a significantly higher frequency of nail dystrophy in this aging study; however, similar lesions were observed infrequently in the MRL/MpJ, FVB/NJ, C57BL/6J, C57BR/cdJ, KK/HIJ, and SWR/J strains, which suggests these nail abnormalities are an age-related change in mice. Weight loss suggests that these injuries may affect feeding and

therefore other experimental parameters in aging studies. All mice in family Group 3 (**Supplemental Table 1**) were affected to some degree which was not the case for any of the other mouse family groups. There was a female predilection in the two most frequently affected strains, NON/ShiLtJ and NZW/LacJ. In no strain were all individuals affected, in contrast to nail unit lesions described in mice with single gene mutations.(4) When blocks that were considered to be non-diagnostic were recut, these observations remained the same.

We considered whether the nail lesions might represent sporadic disease and if it might be considered as a trivial secondary phenotype. The statistical tests undertaken indicate a strongly significant overrepresentation of these lesions in a subset of strains (NON/ShiLtJ and NZW/LacJ) and in at least one strain a sexual dichotomy revealed by the very stringent Fisher's exact test. We consider that dismissal of the phenotype as 'sporadic' or "environmental" previously may well explain its absence from the literature.

Behavioral issues, while not noticed by those working with these strains, can be an underlying cause or predisposition for these types of nail abnormalities. There are examples of mice that self-traumatize for a variety of reasons. Barbering is an abnormal behavior in C57BL/6 and related strains leading to abnormal hair and vibrissae loss and is viewed as model of trichotillomania and obsessive-compulsive spectrum disorders.(22-24) Specific to nail lesions, C57BL/6J mice carrying the *Ngfr<sup>tm1Jae</sup>/J* mutation have decreased peripheral sensory innervation in their footpads. They have decreased sensitivity to pain and other sensations like heat, as a result, which leads them to traumatize their digits and nails as evidenced by ulcerations and secondary infections.(4, 25) These mutant mice develop severe progressive lesions that involve the entire digit without evidence of normal nail regeneration. When consulting with NON/ShiLtJ researchers at The Jackson Laboratory, no abnormal behaviors were observed with these mice. Little was found in the literature on NON/ShiLtJ behavior other than low empathic fear levels.(26)

Phenotypic dependence (i.e. different "orders" of phenotype) is seen in almost all measured phenotypes, especially if a molecular phenotype is seen as the ultimate level of explanation, and yet many measurable traits are the emergent properties of multiple underlying processes, each of which can be assessed separately. We consider that identification of the genetic dependency of any phenotypic trait is sufficient to indicate a potentially tractable etiological mechanism.

We also point out that as with tooth lesions, nail lesions may produce secondary effects themselves which can impact on nutritional status and growth phenotypes. These are often complex phenotypes, especially in mutant strains, and understanding contributory components can help in elucidating their origins in different strains, which could be mechanistically quite different,

While there are no obvious human aging diseases of the nails that resemble what these mice develop, laminitis in ungulates (horses, donkeys, cows, etc.) does have many similarities. Laminitis may have a genetic basis in some breeds.(27) Rotational laminitis is described as rotation and dropping of the distal phalanx within the hoof due to separation of the primary and secondary lamellae which attach the bone to the hoof wall.(28, 29) In some cases, the distal phalanx can penetrate through the bottom of the hoof (pododermatitis circumscripta)(30-32) similar that described in old mice. Although mice lack lamellae attachments of the nail to the distal phalanx, causes of laminitis, such as obesity, metabolic disease, and inflammatory disease should be considered. Analysis of the weights at the time of necropsy of the affected mice revealed that they actually weighed equal to or less on average than the unaffected animals. The



more severely affected mice could have had difficulty getting at the food hoppers, thereby reducing food intake.

Subungual intraosseous epidermoid cysts affecting the distal phalanx are rare lesions reported in humans,(33-37) dogs,(38) and horses.(39) In all species these lesions are usually considered to be reactive or post-traumatic pseudotumors.(35) In the mouse cases, all but one, which had very subtle lesions, exhibited reorganization of the distal phalangeal bone but with no associated inflammation or evidence of active remodeling. Most cysts formed from down-growths of the nail bed which suggest that these lesions may not be trauma-induced, but rather benign proliferative changes of the nail bed.

All nails are usually affected in genetic based nail diseases in inbred mice.(4) In this large scale screen of 30 genetically diverse inbred strains it was assumed at the onset that any nail lesions observed would involve all the digits. This was not the case for nail dystrophy in old mice. It is possible that subungual intraosseous epidermoid cysts may be more common in old mice if all nails were systematically examined. Subungual intraosseous epidermoid cysts need to be recognized as an infrequent, spontaneous lesion in mice when phenotyping new mutant strains.

In summary we report a detailed histopathological analysis and genetic dependency of nail lesions not previously reported in inbred strains of mice. Appreciating the increased frequency in these strains is important when undertaking phenotyping for other purposes and may, due to its genetic dependency, provide a route to the mechanism of the underlying predisposition in these strains.

## Figure legends

**Fig. 1.** A normal nail unit from an unaffected 624 day old male C57L/J mouse illustrates the normal anatomy and terms.

**Fig. 2.** Column one represents an unaffected 624 day old male C57L/J mouse (same as figure 1) to illustrate the normal anatomy of the nail unit (A), at the level of the proximal nail fold and nail matrix (B), the distal tip of P3 with surrounding tissues (C), the hyponychium (D), and P3 to reveal essentially no osteoclasts (E). Column two illustrates a subacutely affected 211 day old male NON/ShiLtJ mouse nail (F-J). Image F shows the protrusion of P3 with inflammation resulting in pressure necrosis of the surrounding tissues beneath the nail plate. The nail matrix is hyperplastic with a hypereosinophilic nail bed (G). The protruding tip of P3 is surrounded by necrotic debris and desiccated proteinaceous material (H). The surrounding tissue is also inflamed (H). The nail bed is hyperplastic with an increased number of mitotic figures as well as a nail bed that appears to be similar to cornified epithelium (I). P3 is undergoing remodeling characterized by an increased number of osteoclasts (J). Column 3 is a chronically affected 406 day old female NON/ShiLtJ mouse (K-O). Fibrotic connective tissue surrounds P3 with significant osteolysis and bone remodeling (K). The proximal nail fold is metaplastic which appears to be an extension of the proximal nail fold epithelium (L). The distal end of the nail unit has a hyperplastic nail bed with a hypereosinophilic nail plate and no defined hyponychium (M). The underlying connective tissue is fibrotic with accumulation of desiccated inflammatory cells under the metaplastic nail plate (N). P3 is undergoing significant remodeling and osteolysis (O). P3 is outlined in dots in A, F, and K.

**Fig. 3.** The nail unit was completely missing from some of the older mice (A; black arrow; 220 day old female NON/ShiLtJ). A scanning electron micrograph reveals one nail unit is missing from a digit (B, white arrow). The lateral side of the nail plate, in a 309 day old female C57BL/6J mouse, had normal flat squames producing a relatively flat and uniform surface (C). By contrast, a 211 day old male NON/ShiLtJ mouse had the lateral side of the nail plate with linear deformities (D).

**Fig. 4.** Subungual intraosseous epidermoid cysts in old mice. A 624 day old BALB/cByJ female mouse nail bed was moderately hyperplastic with papillary projections into the underlying connective tissue with small cyst formations (A, B). Short papillary downgrowths from the nail bed (arrows) with formation of stratified squamous epithelial lined cysts filled with cornified material was an incidental finding in a 623 day old C57L/J mouse (C, D). A 511 day old MRL/MpJ female mouse had several isolated cysts lined by keratinocytes and filled with cornified material with no apparent continuity with the nail bed (E, F). All three cases had remodeling of the bone of P3 from its normal triangular shape.

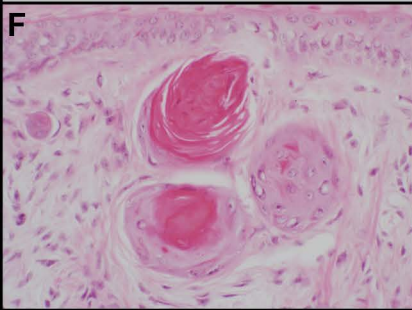
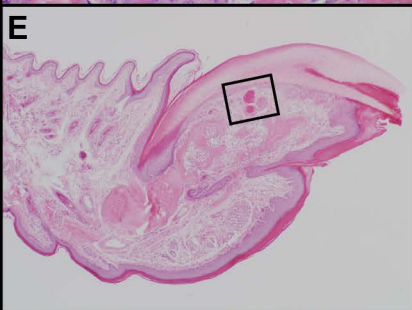
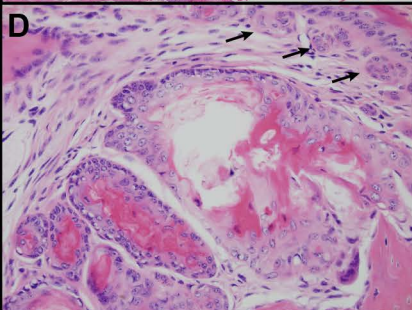
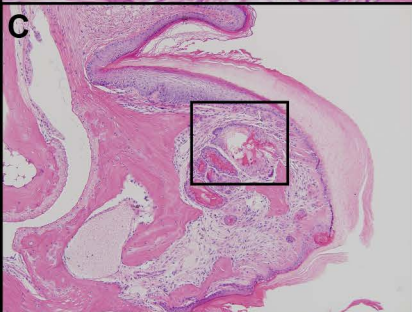
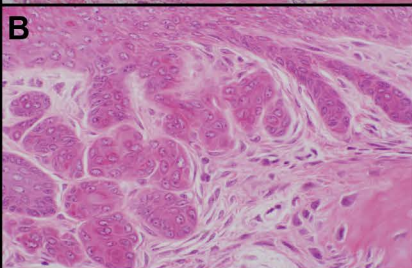
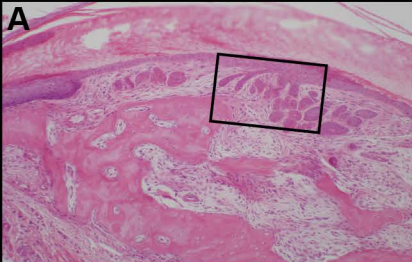
**Table 1.** Number of cases with dystrophy or P3 protrusion/total number of diagnostic nail slides in affected inbred mouse strains.

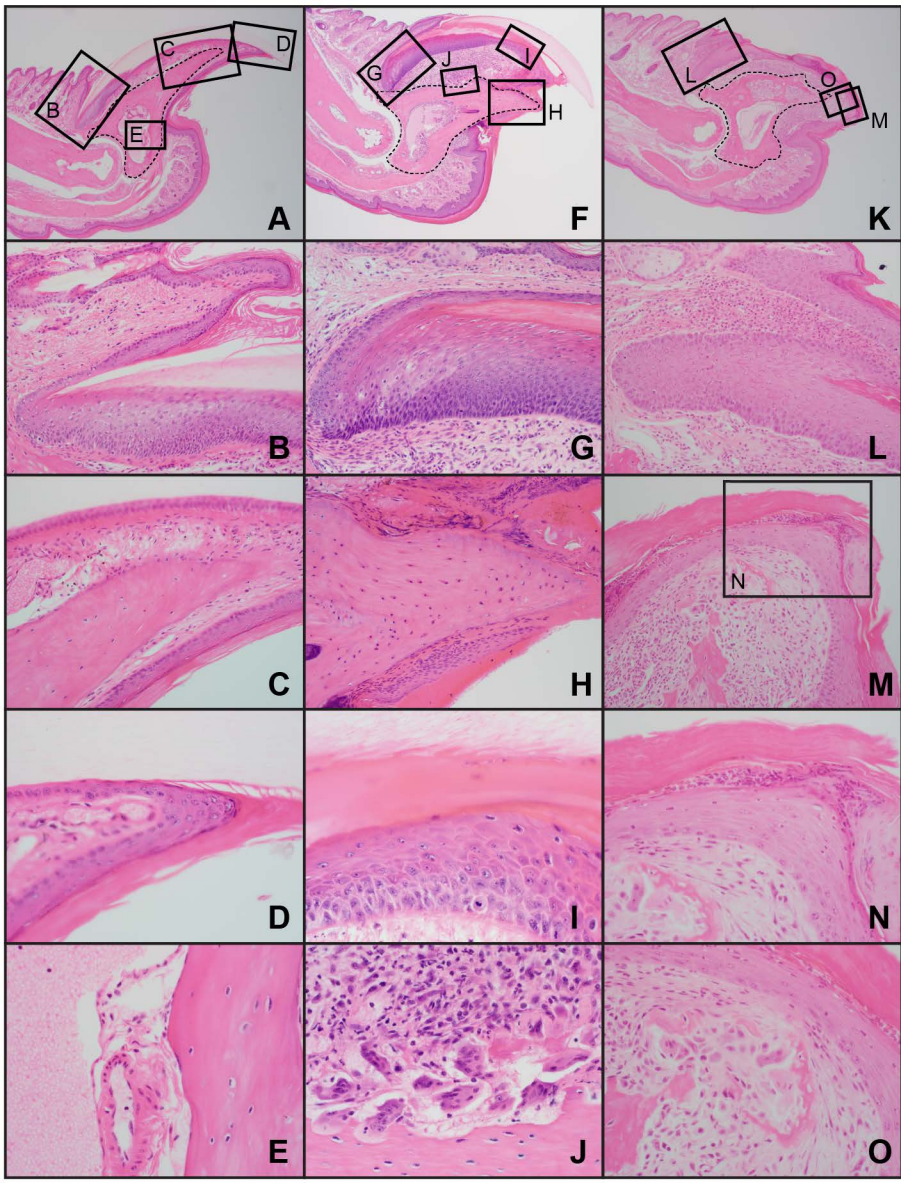
<b>Strain</b>	<b>Sex</b>	<b>12-month-old</b>	<b>20-month-old</b>	<b>&gt;20 month old</b>
C57BL/6J	Fe	0/7	0/5	0/1
C57BL/6J	M	1/10	0/4	1/5
C57BR/cdJ	Fe	0/5	1/9	0/2
C57BR/cdJ	M	1/7	0/10	1/1
FVB/NJ	Fe	0/9	1/4	0/2
FVB/NJ	M	2/11	0/2	0/2
KK/HIJ	Fe	1/6	1/2	0/0
KK/HIJ	M	0/3	0/3	0/1
MRL/MpJ	Fe	1/14	1/9	0/0
MRL/MpJ	M	0/4	0/3	0/0
NON/ShiLtJ	Fe	9/12	12/12	6/6
NON/ShiLtJ	M	5/10	1/12	2/2
NZO/HILtJ	Fe	2/7	0/5	0/0
NZO/HILtJ	M	2/5	0/3	0/0
NZW/LacJ	Fe	4/6	2/3	0/0
NZW/LacJ	M	1/8	0/5	0/1
SM/J	Fe	0/7	0/7	0/0
SM/J	M	0/5	1/8	1/3
SWR/J	Fe	0/11	0/3	0/1
SWR/J	M	0/3	0/4	1/1

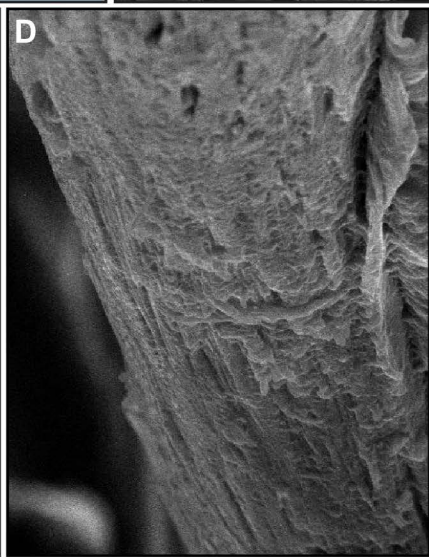
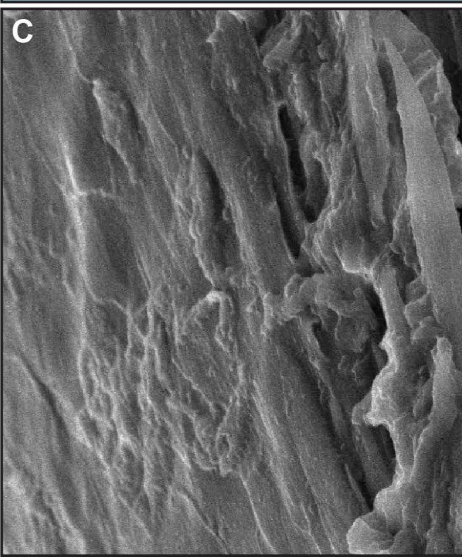
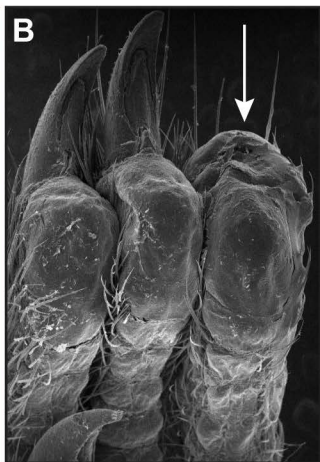
## References

1. Fleckman P, Jaeger K, Silva K A, et al. Comparative anatomy of mouse and human nail units. *Anat Rec (Hoboken)* 2013; 296: 521-532.
2. Crew F A E, Mirskaia L. The character "hairless" in the mouse. *J Genet* 1931; 25: 17-24.
3. Sundberg J P, Dunstan R W, Compton J G. Hairless mouse, HRS/J *hr/hr*. In: Jones T C, Mohr U, Hunt R D, eds. *Integument and Mammary Glands Monographs on Pathology of Laboratory Animals*. Heidelberg: Springer-Verlag, 1989: 192-197.
4. Sundberg J P, King Jr. L E. Skin and its appendages: normal anatomy and pathology of spontaneous, transgenic, and targeted mutant mice. In: Ward J M, Mahler J F, Maronpot R R, et al., eds. *Pathology of genetically engineered mice*. Ames, IA: Iowa State University Press, 2000: 183-215.
5. McElwee K J, Boggess D, Miller J, et al. Spontaneous alopecia areata-like hair loss in one congenic and seven inbred laboratory mouse strains. *J Invest Dermatol Symp Proc* 1999; 4: 202-206.
6. Mecklenburg L, Paus R, Halata Z, et al. FOXP1 is critical for onycholemmal terminal differentiation in nude (*Foxn1*) mice. *J Invest Dermatol* 2004; 123: 1001-1011.
7. Mishina Y, Hanks M C, Miura S, et al. Generation of Bmpr/Alk3 conditional knockout mice. *Genesis* 2002; 32: 69-72.
8. Leung Y, Kandyba E, Chen Y B, et al. Bifunctional ectodermal stem cells around the nail display dual fate homeostasis and adaptive wounding response toward nail regeneration. *Proc Natl Acad Sci USA* 2014; 111: 15114-15119.
9. Sundberg J P, Berndt A, Sundberg B A, et al. The mouse as a model for understanding chronic diseases of aging: the histopathologic basis of aging in inbred mice. *Pathobiol Aging Age Rel Dis* 2011; 1.
10. Sundberg J P, Berndt A, Sundberg B A, et al. Approaches to investigating complex genetic traits in a large-scale inbred mouse aging study. *Vet Pathol* 2016; 53: 456-467.
11. Petkov P M, Ding Y, Cassell M A, et al. An efficient SNP system for mouse genome scanning and elucidating strain relationships. *Genome Res* 2004; 14: 1806-1811.
12. Yuan R, Tsaih S W, Petkova S B, et al. Aging in inbred strains of mice: study design and interim report on median lifespans and circulating IGF1 levels. *Aging Cell* 2009; 8: 277-287.
13. Silva K, Sundberg J P. Necropsy methods. In: Hedrich H J, ed. *The laboratory mouse*. Amsterdam: AP, Elsevier, 2012: 779-806 p.
14. Bechtold L S. Ultrastructural evaluation of mouse mutations. In: Sundberg J P, Boggess D, eds. *Systematic characterization of mouse mutations*. Boca Raton: CRC Press, 2000: 121-129.
15. Sundberg J P, Sundberg B A, Schofield P. Integrating mouse anatomy and pathology ontologies into a phenotyping database: tools for data capture and training. *Mam Genome* 2008; 19: 413-419.
16. Hayamizu T F, Mangan M, Corradi J P, et al. The Adult Mouse Anatomical Dictionary: a tool for annotating and integrating data. *Genome Biol* 2005; 6: R29.
17. Schofield P N, Sundberg J P, Sundberg B A, et al. The mouse pathology ontology, MPATH; structure and applications. *J Biomed Semantics* 2013; 4: 18.
18. Glimm B, Horrocks I, Motik B, et al. HermiT: An OWL 2 Reasoner. *J Automated Reasoning* 2014; 53: 245-269.
19. Hoehndorf R, Hancock J M, Hardy N W, et al. Analyzing gene expression data in mice with the Neuro Behavior Ontology. *Mam Genome* 2014; 25: 32-40.

20. Prüfer K, Muetzel B, Do H-H, et al. FUNC: a package for detecting significant associations between gene sets and ontological annotations. *BMC Bioinformatics* 2007; 8: 41-41.
21. Yekutieli D, Benjamini Y. Resampling-based false discovery rate controlling multiple test procedures for correlated test statistics. *J Stat Plan Inf* 1999; 82: 171-196.
22. Sundberg J P, Brown K S, McMahon W M. Chronic ulcerative dermatitis in black mice. In: Sundberg J P, ed. *Handbook of mouse mutations with skin and hair abnormalities Animal models and biomedical tools*. Boca Raton, FL: CRC Press, 1994: 485-492.
23. McMahon W M, Sundberg J P. Barbering behavior abnormalities in inbred laboratory mice. In: Sundberg J P, ed. *Handbook of mouse mutations with skin and hair abnormalities Animal models and biomedical tools*. Boca Raton, FL: CRC Press, 1994: 493-497.
24. Garner J P, Weisker S M, Dufour B, et al. Barbering (fur and whisker trimming) by laboratory mice as a model of human trichotillomania and obsessive-compulsive spectrum disorders. *Comp Med* 2004; 54: 216-224.
25. Lee K F, Li E, Huber L J, et al. Targeted mutation of the gene encoding the low affinity NGF receptor p75 leads to deficits in the peripheral sensory nervous system. *Cell* 1992; 69: 737-749.
26. Keum S, Park J, Kim A, et al. Variability in empathic fear response among 11 inbred strains of mice. *Genes Brain Behav* 2016; 15: 231-242.
27. Lewis S L, Holl H M, Streeter C, et al. Genomewide association study reveals a risk locus for equine metabolic syndrome in the Arabian horse. *J Anim Sci* 2017; 95: 1071-1079.
28. Aguirre C N, Talavera J, Fernandez Del Palacio M J. Usefulness of Doppler ultrasonography to assess digital vascular dynamics in horses with systemic inflammatory response syndrome or laminitis. *J Am Vet Med Assoc* 2013; 243: 1756-1761.
29. Parks A H. Structural dynamics of displacement of the distal phalanx. In: Belknap J K, Geor R, eds. *Equine laminitis*. Hoboken, N.J.: John Wiley & Sons, 2017: 176-180.
30. Gantke S, Nuss K, Köstlin R. Radiologic findings in bovine laminitis. *Tierarztl Prax Ausg G Grosstiere Nutztiere* 1998; 26: 239-246.
31. van Amstel S R, Shearer J K. Review of Pododermatitis circumscripta (ulceration of the sole) in dairy cows. *J Vet Intern Med* 2006; 20: 805-811.
32. Birkeland R, Fjeldaas T. Diseases in the distal extremities of cows--a pathoanatomical study. *Nord Vet Med* 1984; 36: 145-155.
33. Wang B Y, Eisler J, Springfield D, et al. Intraosseous epidermoid inclusion cyst in a great toe. A case report and review of the literature. *Arch Pathol Lab Med* 2003; 127: e298-300.
34. Connolly J E, Ratcliffe N R. Intraosseous epidermoid inclusion cyst presenting as a paronychia of the hallux. *J Am Podiatr Med Assoc* 2010; 100: 133-137.
35. Van Tongel A, De Paepe P, Berghs B. Epidermoid cyst of the phalanx of the finger caused by nail biting. *J Plast Surg Hand Surg* 2012; 46: 450-451.
36. Shin J J, Kwon K Y, Oh J R. Intraosseous epidermoid cyst discovered in the distal phalanx of a thumb: a case report. *Hand Surg* 2014; 19: 265-267.
37. Park I J, Kim H M, Lee J Y, et al. An intraosseous epidermal cyst developing in a metacarpal bone after K-wire fixation: a case report. *Skeletal Radiol* 2015; 44: 1523-1527.
38. Frank H, Kirchhof N, Biesenbach W, et al. [Intraosseous epidermoid cysts of the toe phalanx in dogs]. *Berl Munch Tierarztl Wochenschr* 1995; 108: 73-76.
39. Headley S A, Kummala E, Saarinen H, et al. Diagnostic exercise: intraosseous epidermoid cysts in the third phalanx of a dressage mare. *Vet Pathol* 2009; 46: 355-357.









Proximal Nail Fold

Cuticle

Nail Plate

Nail Bed

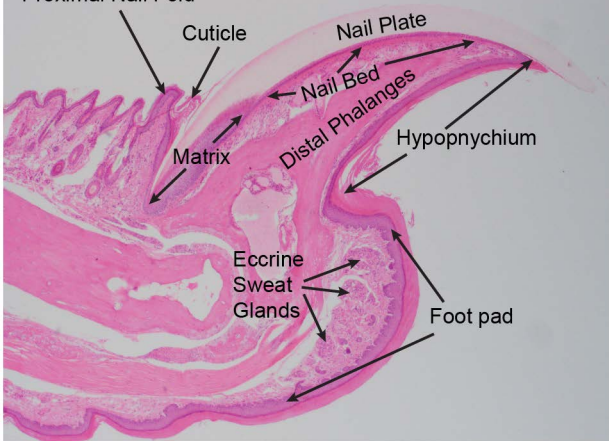
Matrix

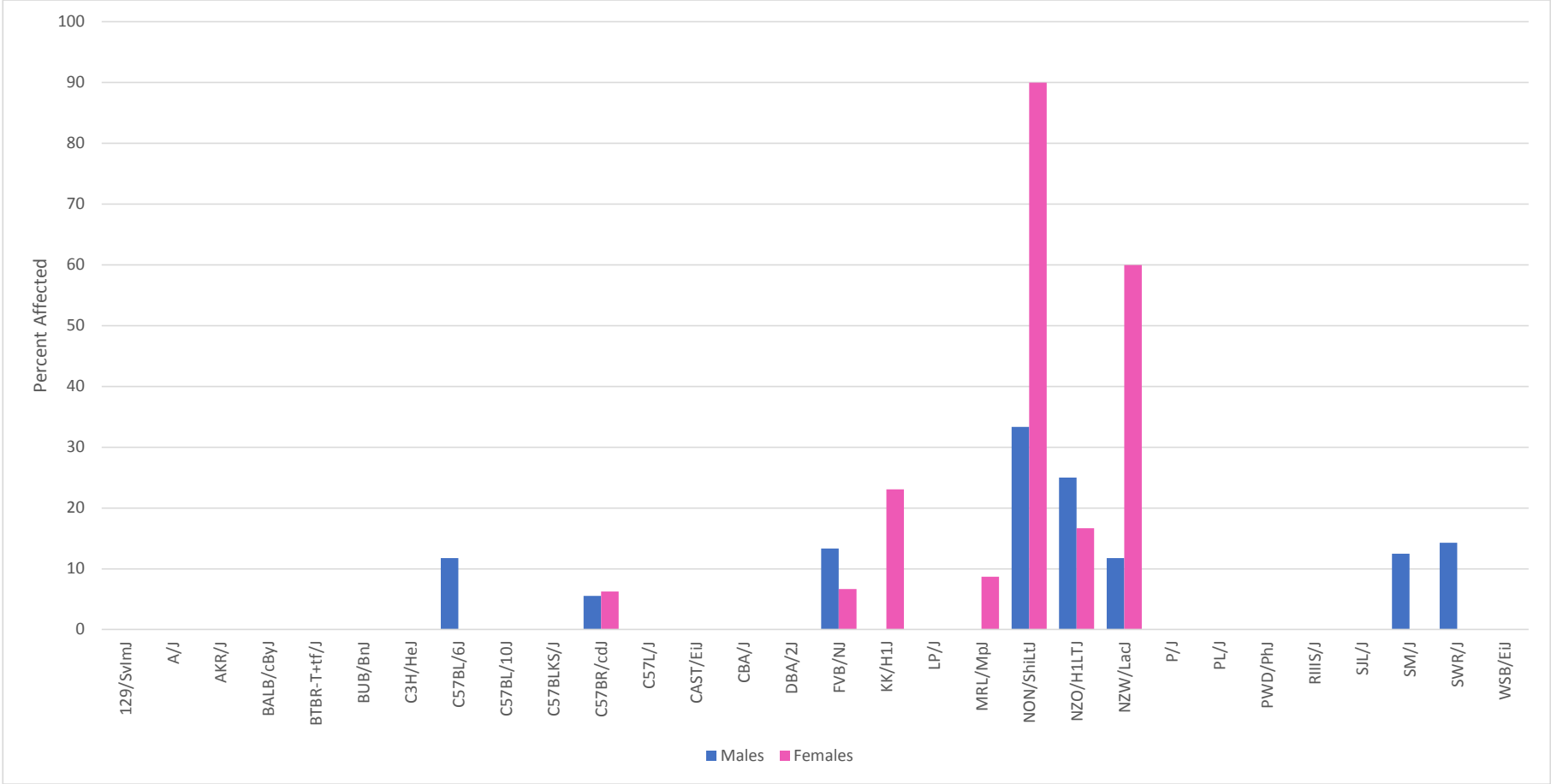
Distal Phalanges

Hypopnuchium

Eccrine  
Sweat  
Glands

Foot pad





## Supplemental Data

**Supplemental Table 1.** Mouse family tree groupings of mice used in the aging study.(1) Strains with nail dystrophy are in bold type and the two with the highest frequency are highlighted in brown. Note all mouse strains in Group 3 have the nail abnormality suggesting an hereditary propensity.

Group 1	Group 2	Group 3	Group 4	Group 5	Group 6	Group 7
A/J	BUB/BnJ	<b>KK/HlJ</b>	<b>C57BL/6J</b>	129S1/SvImJ	DBA/2J	CAST/EiJ
AKR/J	<b>FVB/NJ</b>	<b>NON/ShiLtJ</b>	C57BL/10J	BTBR T <sup>+</sup>	P/J	PWD/PhJ
BALB/cByJ	NOD.B10Sn	<b>NZO/HILtJ</b>	C57BLKS/J	LP/J	<b>SM/J</b>	WSB/EiJ
C3H/HeJ	RISS/J	<b>NZW/LacJ</b>	<b>C57BR/cdJ</b>			
CBA/J	SJL/J		C57L/J			
<b>MRL/MpJ</b>	<b>SWR/J</b>					
PL/J						

<b>Supplemental Table 2.</b> Summary of mice affected with subungual intraosseous epidermoid cysts.		
Strain	Sex	Age (days)
129S1/SvImJ	Male	798
BALB/cByJ	Male	624
C57L/J	Male	377
C57L/J	Male	623
FVB/NJ	Female	760
FVB/NJ	Male	882
LP/J	Male	826
MRL/MpJ	Female	511

## References

1. Petkov P M, Ding Y, Cassell M A, et al. An efficient SNP system for mouse genome scanning and elucidating strain relationships. *Genome Res* 2004; 14: 1806-1811.

**Supplemental Figure 1.** Distribution of nail dystrophy or perforation of P3 in 30 inbred strains at 12, 20, and greater than 20 months of age. Raw numbers suggested that NON/ShiLtJ and NZW/LacJ females were most frequently affected. Estimation of significance based on Fisher's Exact test indicated that females were most frequently affected in NON/ShiLtJ at 20 months ( $p=1e-5$ ) but NZW/LacJ failed to reach significance ( $p=0.05$ ) for sexual dichotomy at either time point (12 months  $p=0.09$ , 20 months  $p=0.107$ ).

